Directed transport induced by asymmetric surface vibrations: making use of friction

2007 J. Phys.: Condens. Matter 19 096004

(http://iopscience.iop.org/0953-8984/19/9/096004)

IOP PUBLISHING JOURNAL OF PHYSICS: CONDENSED MATTER

J. Phys.: Condens. Matter **19** (2007) 096004 (8pp) doi:10.1088/0953-8984/19/9/096004

Directed transport induced by asymmetric surface vibrations: making use of friction

D Fleishman, Y Asscher and M Urbakh

School of Chemistry, Tel Aviv University, 69978 Tel Aviv, Israel

Received 15 August 2006, in final form 14 December 2006
Published 12 February 2007
Online at stacks.iop.org/JPhysCM/19/096004

Abstract

It is shown that making use of frictional interactions allows for an effective directed motion of a block produced by asymmetrical vibrations of the underlying plate. We found that the block dynamics exhibits four different regimes of motion depending on the relationships between the values of the frictional forces and the characteristics of the plate vibrations. The optimal motion of the block can be achieved by tuning the amplitudes and frequencies of the vibrations in a controllable way.

1. Introduction

The origin of transport in dynamical systems at atomic and mesoscales has been an active research area during recent years. It was found that nonlinear interactions may lead to many intriguing dynamical features of these systems, in particular to directed transport, which is produced by breaking time and/or spatial symmetries, without applying an external constant bias [1–8]. Most studies have focused on the classical dynamics of a particle or a chain of particles in a one-dimensional periodic potential under the influence of a time-periodic external field [1–7]. The mechanism of directed motion in these systems has been studied in detail. It has been shown that directed motion can be induced dynamically and no spatial asymmetry is required which is built into the system [4–6, 8]. In contrast, the dynamics of mesoscopic objects (of micrometre size) driven by time-dependent forces with a zero mean has attracted less attention, although it offers new directions in microfluidics and micromachining applications [9–14]. Asymmetric vibrations of surfaces have been already used to move droplets, hydrogel rods, microparticles and other solid objects on surfaces [9–11, 14, 15].

The motion of a mesoscale object (block) on a solid plate involves the interaction of a large ensemble of asperities that form the frictional interface [16, 17]. This effect gives rise to a static friction (the force necessary to start sliding) and velocity-dependent kinetic friction (the force necessary to keep sliding at a given velocity). Usually such behaviour is referred to as dry friction. The dynamical response of a mechanical system with dry friction is nonlinear because the frictional force in a sliding state differs from the static friction.

In this paper we investigate the motion of a mesoscopic block produced by asymmetrical lateral vibrations of the underlying plate. Qualitative features of the vibration-induced motion have been discussed recently [11]. Here we extend this study by including more realistic laws of friction and investigating in detail possible regimes of the block motion. We demonstrate that making use of frictional interactions allows for an effective directed motion of the block produced by asymmetrical vibrations of the underlying plate. The observed dynamical regimes are strongly dependent on the ratio between the values of the static friction and kinetic friction at low velocities. The direction and velocity of the block are determined by the frequency, amplitude and shape of the prescribed plate vibrations. All these parameters can be tuned to achieve desirable modes of block motion.

2. The model

Let us consider a solid block located on a plate that undergoes asymmetrical lateral vibrations of zero mean force. Interactions between the sliding block and the plate can be described by static friction, F_s, and velocity-dependent kinetic friction, F_k. Here we use the simple form of the kinetic friction

$$F_k = -F_k^0 \mathrm{sgn}(\dot{x}) - \eta\dot{x} \tag{1}$$

where $\dot{x}$ is the velocity of the block with respect to the plate, $\mathrm{sgn}(\dot{x})$ denotes the sign of $\dot{x}$, F_k^0 is the limiting value of kinetic friction at zero velocity and η is a dissipation constant. Equation (1) adequately depicts the frictional properties of solid systems at the scale above tenths of nanometres [16].

It is convenient to write an equation of motion in the reference frame of the vibrating plate. For the equation of motion we have to distinguish whether the block sticks with the plate or slips. If it sticks, its position relative to the plate, x, does not change until the driving force, F_{in}, exceeds the static friction. Thus

$$\dot{x} = 0 \qquad \text{if } |F_{in}| \leqslant F_s. \tag{2}$$

If the block slips, the equation of motion reads

$$m\ddot{x} = F_k + F_{in} \tag{3}$$

where the driving force presents the effects of inertia $F_{in} = -m\mathrm{d}^2x_{pl}/\mathrm{d}t^2$, m is the block mass and $x_{pl}(t)$ is the plate coordinate. It should be noted that inertial forces are used to create dynamic motion for coarse positioning in commercial scanning probe instruments [15]. In this work we consider a case of biharmonic driving when the plate vibrations have the following form:

$$x_{pl} = A_1\cos(\omega_1 t + \varphi_1) + A_2\cos(\omega_2 t + \varphi_2). \tag{4}$$

Most of results presented below have been obtained for

$$A_2 = A_1/2 > 0, \qquad \omega_2 = 2\omega_1, \qquad \varphi_1 = \varphi_2 = 0.$$

It is convenient to introduce dimensionless coordinates and time, $\tilde{x} = x/A_1$ and $\tilde{t} = t/\tau$, where $\tau = 2\pi/\omega_1$. The dynamical behaviour of the system is determined by the following dimensionless parameters: $r = F_k^0/F_s$, $\tilde{\eta} = \eta\tau/m$, $\tilde{F}_s = F_s/(A_1 m\omega_1^2)$ and $\tilde{F}_{in} = F_{in}/(A_1 m\omega_1^2)$. In order to characterize the block motion we performed numerical calculations over 200 periods of oscillations and present dependences of the mean block displacement during one period of vibrations, X, and the drift velocity $V = X/\tau$ on system parameters. In the following we refer to X as the net drift.

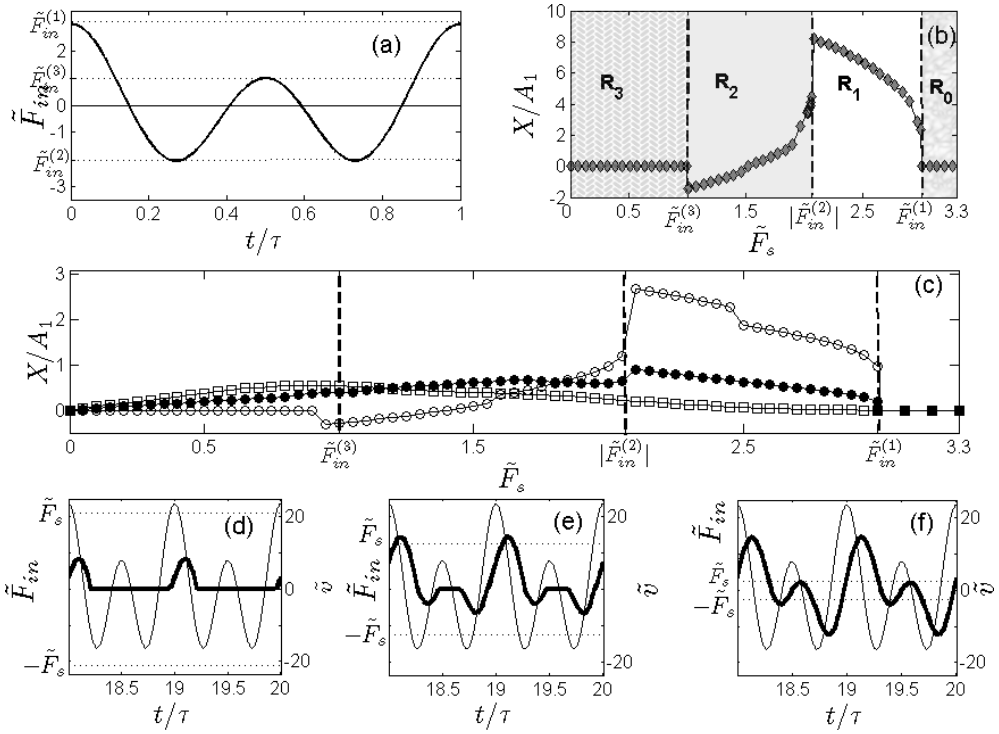

Figure 1. (a) Time dependence of the driving force, $\tilde{F}_{\rm in}(t)$. The dotted lines show acceleration, $\tilde{F}_{\rm in}^{(1)}$ and $\tilde{F}_{\rm in}^{(3)}$, and deceleration, $\tilde{F}_{\rm in}^{(2)}$, peaks respectively. ((b), (c)) Dimensionless net drift of the block, $\tilde{X} = X/A_1$, as a function of dimensionless static friction: (b) $F_{\rm k}^0 = 0$, $\eta = 0$; (c) $\tilde{\eta} = 1$ and $F_{\rm k}^0/F_{\rm s} = 0$ (——○——), 0.5 (——●——) and 1 (——□——). Other parameters: $A_1/A_2 = 2$, $\omega_2/\omega_1 = 2$. Four regimes of motion observed at low kinetic friction are marked as R_0, R_1, R_2 and R_3. The boundaries between these regimes which were found for $F_{\rm k}^0 = 0$, $\eta = 0$ (equation (6)) are shown by dashed lines. ((d)–(f)) Time dependences of the dimensionless block velocity, $\tilde{v} = \dot{x}(t)/(A_1/\tau)$, (bold solid lines) for three regimes of motion: (c) R_1 ($\tilde{F}_{\rm s} = 2.90$), (d) R_2 ($\tilde{F}_{\rm s} = 1.58$) and (e) R_3 ($\tilde{F}_{\rm s} = 0.95$). Thin solid lines show the driving force, and dotted lines show the values of the static friction, $\pm\tilde{F}_{\rm s}$. Here $F_{\rm k}^0 = 0$ and the other parameters are as in (c).

It should be noted that equations (1)–(4) can be solved analytically, but the resulting expressions are too cumbersome and we do not present them here. Below we present the results of numerical calculations, discuss typical regimes of motion induced by the biharmonic driving, and demonstrate how this motion can be tuned varying the amplitude and frequency of the plate vibrations.

As we show below, the driving force, $F_{\rm in}$, with zero average can induce a directed motion of the block only in the presence of nonzero static or kinetic friction, $F_{\rm k}^0$. In order to get nonzero drift velocity the duration of the prescribed plate motion with positive acceleration should be different from that with negative acceleration (see figure 1(a)).

3. Results and discussion

We found that the observed regimes of the block motion are mainly determined by relationships between the peak values of the driving force and the value of the static friction. For the force profile in figure 1(a) there are two acceleration peaks, $F_{\rm in}^{(1)}$ and $F_{\rm in}^{(3)}$, and a deceleration peak,

$F_{\rm in}^{(2)}$, whose amplitudes are given by the following equations:

$$\begin{aligned} F_{\rm in}^{(1)} &= m\omega_1^2(A_1 + 4A_2), \qquad F_{\rm in}^{(3)} = m\omega_1^2(4A_2 - A_1), \\ F_{\rm in}^{(2)} &= -m\omega_1^2(A_1^2/32A_2 + 4A_2). \end{aligned} \tag{5}$$

It should be noted that $F_{\rm in}^{(1)} > |F_{\rm in}^{(2)}| > F_{\rm in}^{(3)}$. Figures 1(b) and (c) show the dependences of the block net drift, $\tilde{X}$, on the static friction for given driving parameters and a given ratio between the static and kinetic friction, $F_{\rm k}^0/F_{\rm s}$. One can see that in the case of low kinetic friction, $F_{\rm k}^0 < 0.5F_{\rm s}$, four regimes of motion can be isolated, which we denote $R_0 - R_3$. In the idealized case of a negligible kinetic friction, $F_{\rm k}^0 = \eta = 0$, the positions of the boundaries between the regimes are determined by the three peak magnitudes of $F_{\rm in}$ (see figure 1(b)) and can be calculated as

$$F_{\rm s} = F_{\rm in}^{(i)}, \qquad i = 1, 2, 3. \tag{6}$$

Figure 1(c) shows that, in a realistic case of nonzero kinetic friction, the boundaries between the different regimes of motion are slightly shifted from the values given by equation (6), but the general features of the dynamics remain the same as for $F_{\rm k}^0 = \eta = 0$.

In the first regime R_0, where $\tilde{F}_{\rm in}^{(1)} \leqslant \tilde{F}_{\rm s}$, the driving force is always lower than the static friction and the block remains stuck to the plate. In the regime R_1, which for $F_{\rm k}^0 = \eta = 0$ occurs at $|\tilde{F}_{\rm in}^{(2)}| \leqslant \tilde{F}_{\rm s} < \tilde{F}_{\rm in}^{(1)}$, the vibrations of the plate induce one 'burst' of block motion in the positive direction (see figure 1(d)), and a reduction of the static friction for a given driving force leads to an increase of the net drift $\tilde{X}$ (see figures 1(b) and (c)). In the regime R_2 ($\tilde{F}_{\rm in}^{(3)} \leqslant \tilde{F}_{\rm s} < |\tilde{F}_{\rm in}^{(2)}|$ for $F_{\rm k}^0 = \eta = 0$), which can be called a 'two-burst regime'; the block motion in the negative direction becomes also possible (see figure 1(e)), and time intervals of negative displacement increase with a reduction of $\tilde{F}_{\rm s}$. As a result, the drift, $\tilde{X}$, in the regime R_2 is smaller than that in R_1 (see figures 1(b) and (c)). It should be noted that the inversion of the drift velocity with a variation of $\tilde{F}_{\rm s}$ can be observed in this regime.

The dynamics in regimes R_2 and R_3 can be represented as a set of the alternating segments of stick or slip motion of the block. In contrast, the regime of low static friction, R_3 ($\tilde{F}_{\rm s} < \tilde{F}_{\rm in}^{(3)}$ for $F_{\rm k}^0 = \eta = 0$), does not show sticking intervals (see figure 1(f)). Here the driving force acting on the block at the turning points of its motion is always higher than the static friction, and the block never stops. In this regime the static friction is of no importance, and it is the kinetic friction that breaks the symmetry of the block motion and leads to a nonzero net displacement. As expected, the latter vanishes for $F_{\rm s}, F_{\rm k}^0 \to 0$.

Figure 1(c) shows that an increase of kinetic friction ($F_{\rm k}^0$ and η) smears the boundaries between different regimes of motion. In particular, for $F_{\rm k}^0 > 0.5F_{\rm s}$ and $\tilde{\eta} \gg 1$ the bursts of motion in the negative direction, which are characteristic for the regimes $R_{2,3}$, give only minor contribution to the net drift, and as a result we do not observe a decrease of $\tilde{X}$ when passing from regime R_1 to the regimes $R_{2,3}$. However, the main features of the vibration-induced motion discussed above for a case of low kinetic friction are still retained for larger values of $F_{\rm k}^0$ and η. These include nonzero net drift for $0 < \tilde{F}_{\rm s} < \tilde{F}_{\rm in}^{(1)}$, alternating segments of stick and slip motion of the block and more.

Figure 2 demonstrates the effect of kinetic friction on the drift for three typical values of static friction. For high static friction, corresponding to the one-burst regime R_1 (curve ——□—— in figure 2), we found an expected reduction of the drift with increase of $F_{\rm k}^0$. In this regime the block moves in the positive direction only, and under these conditions an increase of the resistant force, $-F_{\rm k}^0{\rm sgn}(\dot{x})$, decreases the overall displacement. In contrast, a counterintuitive increase of the drift with $F_{\rm k}^0$ has been observed for low static friction (curve ——●—— in figure 2). In this regime, R_3, the static friction is of minor importance,

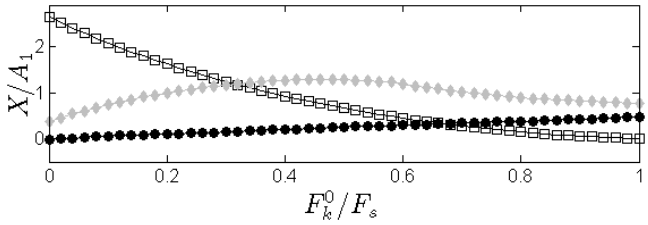

Figure 2. Dimensionless net drift of the block as a function of the dimensionless kinetic friction. The results have been obtained for three values of static friction, $\tilde{F}_s$: 0.95 (——●——), 1.58 (——♦——) and 2.9 (——□——), which correspond to regimes R_1, R_2 and R_3, respectively. The other parameters are as in figure 1(c).

and an increase of the kinetic friction enhances an asymmetry of the block motion and as a result intensifies a directed motion. It has been show recently [11] that in this case the net drift can be estimated as

$$X = -F_k^0 \bar{s}/\eta \tag{7}$$

where $\bar{s} = \int_0^\tau \mathrm{d}t s(t)$ and $s(t)$ is a sign of the block velocity for F_s, $F_k^0 = 0$. The results presented in figure 2 follow equation (7), showing a linear increase of the net drift with F_k^0. In the intermediate two-burst regime R_2 (curve ——♦—— in figure 2) an interplay between the effects of breaking symmetry and an additional resistance leads to a non-monotonic dependence of $\tilde{X}$ on F_k^0. Hence our calculations demonstrate that a relation between the static and dynamic friction strongly affects the efficiency of the vibration-induced motion.

The above analysis allows us to understand the dependence of the drift on the driving parameters (amplitudes A_1 and A_2 and frequencies ω_1, ω_2) and to achieve a desirable mode of motion of the block. Figures 3(a) and (b) show the dependence of the drift on the amplitude A_1, for a given ratio between amplitudes, $A_2/A_1 = 0.5$. The regimes of motion presented in these figures are similar to those shown in figure 1. As above, for reasonable values of kinetic friction, $F_k^0/F_s \leqslant 0.5$, one can distinguish four regimes of motion. In the case of a negligible kinetic friction, $F_k^0 = \eta = 0$, the positions of the boundaries between the regimes are given by solutions of equation (6), and for nonzero kinetic friction the boundaries are slightly shifted from the corresponding values (see figures 3(a) and (b)).

For low kinetic friction the most efficient motion of the block in the positive direction is attained for the value of the amplitude A_1, which corresponds to the boundary between regimes R_1 and R_2, when $|\tilde{F}_{in}^{(2)}| \approx \tilde{F}_s$. The direction of the net drift changes in regime R_2, and the maximal negative drift occurs at a boundary between regimes R_2 and R_3, i.e. when $\tilde{F}_{in}^{(3)} \approx \tilde{F}_s$. It should be noted that the length and duration of the bursts in regimes R_2 and R_3 can be tuned with high precision by changing the amplitude A_1. This may be useful for micromachining applications where high precision positioning requirements are of primary importance.

At high driving amplitudes, $\tilde{F}_{in}^{(3)} \gg \tilde{F}_s$, the block never stops (regime R_3) and the drift levels off at a limiting value as A_1 increases. In this regime the motion is independent of the value of static friction and the net drift is proportional to the kinetic friction, as suggested by equation (7). This behaviour has been examined in detail recently [11], and the results of our calculations are in good agreement with the predictions of that work.

Figure 3(c) demonstrates a possibility to tune the block motion through a variation of the ratio of amplitudes, A_1/A_2, for a given value of A_1. For large and small values of the ratio, $A_1/A_2 \gg 1$ and $A_1/A_2 \ll 1$, the plate motion becomes symmetrical and the net drift is negligible no matter how large the amplitude of the driving force is. To achieve the maximal drift one has to keep the ratio A_1/A_2 close to 0.5.

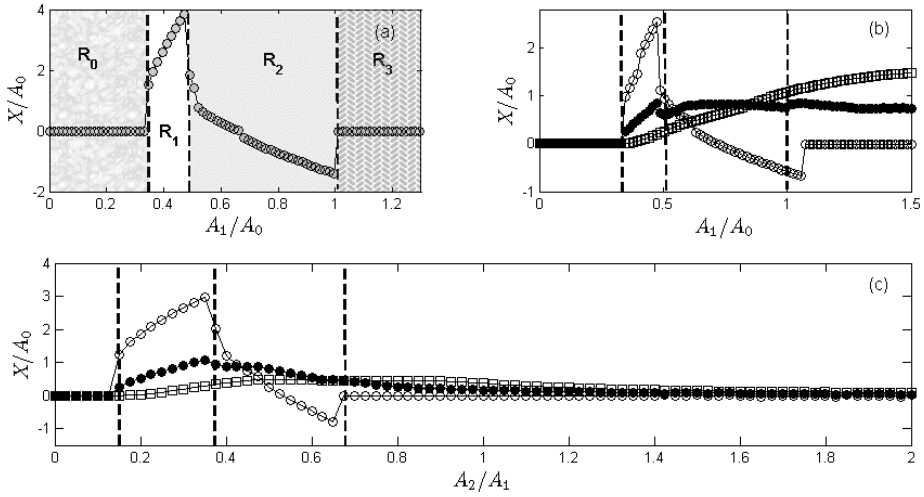

Figure 3. ((a), (b)) Dimensionless net drift of the block as a function of the dimensionless driving amplitude $\tilde{A}_1 = A_1/A_1^0$, where $A_1^0 = F_s/(m\omega_1^2)$. The results have been obtained for a given ratio of the amplitudes $A_1/A_2 = 2, \omega_2/\omega_1 = 2$ and (a) $F_k^0 = 0, \eta = 0$; (b) $\tilde{\eta} = 1$ and three values of kinetic friction, $F_k^0/F_s = 0$ (—○—), 0.5 (—●—), 1 (—□—). (c) Dimensionless net drift of the block as a function of the ratio of the amplitudes A_2/A_1. The results have been obtained for $A_1 = 0.6F_s/(m\omega_1^2)$, $F_k^0/F_s = 0$ (—○—) and 0.5 (—●—). The other parameters are as in figure 1(c). The boundaries between the regimes of motion which were found for $F_k^0 = 0$, $\eta = 0$ (equations (6)) are shown by dashed lines.

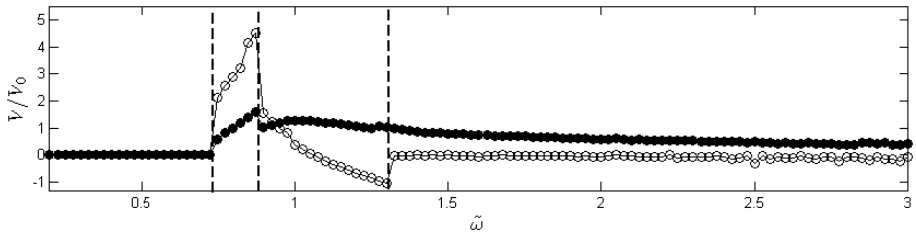

Figure 4. Dimensionless drift velocity, $\tilde{V} = V/V_0$, as a function of the dimensionless driving frequency $\tilde{\omega} = \omega_1/(2\pi\eta m)$, where $V = X/\tau$ and $V_0 = A_1\eta/m$. The results have been obtained for two values of kinetic friction F_k^0/F_s: 0 (—○—) and 0.5 (—●—). The boundaries between the regimes of motion which were found for $F_k^0 = 0$, $\eta = 0$ (equations (6)) are shown by dashed lines. Parameter values: $\omega_2/\omega_1 = 2$, $\tilde{F}_s(\omega_1 = 2\pi\eta/m) = 1.58$.

Another parameter which can be used to achieve a desirable motion of the block is the frequency of vibrations. The dependency of the drift velocity on ω_1 is presented in figure 4. In contrast to previous figures, here we show the drift velocity rather than the displacement since the period of vibrations changes in this case. Two effects determine the dependence of V on ω_1: (i) the amplitude of the driving force is proportional to ω^2, (ii) there is a competition between timescales of external driving, $1/\omega$, and relaxation, m/η. Also here for low kinetic friction, $F_k^0 < 0.5F_s$, the four regimes of motion described above are visible in figure 4. The drift velocity vanishes at both low and high frequencies. In the first case the maximal value of the driving force is smaller than the static friction (regime R_0), and the block is stuck with the plate. At high frequencies the block never stops moving in both positive and negative directions

(regime R_3). However, a duration of displacements in each direction decreases with ω_1, and as a result the drift velocity also vanishes. The maximal drift velocity is achieved at a frequency corresponding to a boundary between regimes R_1 and R_2, and there is an inversion of the direction of the drift velocity in the two-burst regime, R_2. With increase of the kinetic friction the motion in the negative direction is suppressed and velocity inversion disappears; also the maximum of the drift velocity shifts to higher frequencies.

4. Possible experimental implementations

In order to define the values of driving parameters which should be used under realistic conditions one has to know the magnitudes of the static and kinetic friction, F_s, F_k^0, and the dissipation coefficient η. Experimental studies of a wide range of materials indicate that the frictional forces follow the modified Amontons' equation [16]:

$$F_s = \mu_s(F_s^{adh} + L) \tag{8}$$

where μ_s is a static friction coefficient, F_s^{adh} is an adhesive force acting between the block and the underlying surface at rest, and L is a normal load which in our case equals the gravitational force, mg. The above equation accounted for the experimental observation that there is already a finite friction force at zero load for adhering surfaces. A similar equation applies to the kinetic friction

$$F_k^0 = \mu_k(F_k^{adh} + L) \tag{9}$$

where μ_k is a kinetic friction coefficient and F_k^{adh} is an adhesive force in the kinetic state which is smaller than the static adhesive force. It should be noted that for nanosize and microsize systems F_s^{adh}, $F_k^{adh} \gg mg$, and the contribution of the gravitational force to friction can be neglected.

In order to illustrate our theoretical results we use here the data obtained for a microelectromechanical device (MEMS) which presents a microsize silicon block sliding on a monolayer-lubricated polycrystalline silicon surface [18]. For this system $\mu_s \approx 0.33$, $\mu_k \approx 0.24$, $F_s^{adh} = 4.6\ \mu$N, $F_k^{adh} = 4.2\ \mu$N, $\eta/m \approx 10^3\ s^{-1}$ and $mg = 0.03\ \mu$N. Similar friction parameters have been reported for nanoparticles (areas between 10^4 and $10^5\ nm^2$) deposited on graphite and molybdenum disulfide surfaces [19]. Then for the frequency $2\pi\omega_1 = 10$ kHz, which is readily accessible by the shear modulation technique, our calculations show that a directed motion of the block can be induced for the driving amplitudes, $A > 66.5\ \mu$m. For the above values of parameters the maximal drift velocity $V = 57.4 \times 10^{-2}\ m\ s^{-1}$ is achieved in the one-burst regime, R_1, for $A_1 = 95\ \mu$m, and the corresponding burst (step) length equals $57.4\ \mu$m. On varying the amplitude from 66 to 95 μm, one can get a desirable magnitude of the step length ranging from a few nanometres to 100 micrometres. These estimations demonstrate that the proposed mechanism provides long-range motion with step sizes lying in the nanometre to micrometre range. Hence this approach may be useful for very high precision positioning requirements in micromachining applications [13].

Another possible application of the vibration-induced sliding discussed here is a separation of particles deposited on surfaces according to their sizes. The adhesive forces in equations (8) and (9) are proportional to the area of contact between the particle and the surface, while the driving force is proportional to the volume of the particle. As a result, by properly adjusting the driving amplitude and frequency, particles of different sizes may be forced to move with different drift velocities in the same or in opposite directions (see figures 1(b) and (c)). Alternatively, particles of a certain size may be forced to stay localized while others move in a desirable direction with a desirable velocity.

It should also be noted that by measuring the dependence of drift velocity on the amplitude and frequency of vibrations and comparing the results with the theoretical prediction, one can estimate the values of static and kinetic friction which are still not well defined at the microscale and the nanoscale. Hence the proposed approach gives certain access to frictional and adhesional properties of microscale and nanoscale objects that may contribute to a better understanding of the fundamental process of friction.

5. Conclusions

We have demonstrated that, in the presence of nonzero static or/and kinetic friction, effective directed motion of the block can be produced by biharmonic vibrations of the underlying plate. The block dynamics exhibits four different regimes of motion depending on the relationships between the values of frictional forces and the characteristics of the plate vibrations. We have shown that the direction, velocity and length of individual bursts of the block are determined by the frequency, amplitude and shape of the plate vibrations. The optimal motion of the block can be achieved by tuning the driving parameters in a controllable way.

Acknowledgments

This research was supported by the Israel Science Foundation (grant No 1116/05) and by the Deutsche Forschungsgemeinschaft (HA 1517/26-2).

References

[1] Jülicher F, Ajdari A and Prost J 1997 *Rev. Mod. Phys.* **69** 1269
[2] Reimann P 2002 *Phys. Rep.* **361** 57
[3] Astumian R D and Hanggi P 2002 *Phys. Today* **55** 33
[4] Flach S, Yevtushenko O and Zolotaryuk Y 2000 *Phys. Rev. Lett.* **84** 2358
[5] Porto M, Urbakh M and Klafter J 2000 *Phys. Rev. Lett.* **85** 491
[6] Denisov S, Klafter J, Urbakh M and Flach S 2002 *Physica* D **170** 131
[7] Borromeo M, Hanggi P and Marchesoni F 2005 *J. Phys.: Condens. Matter* **17** S3709
[8] Fleishman D, Filippov A E and Urbakh M 2004 *Phys. Rev.* E **69** 011908
[9] Daniel S, Chaudhury M K and de Gennes P-G 2005 *Langmuir* **21** 4240
[10] Mahadevan L, Daniel S and Chaudhury M K 2004 *Proc. Natl Acad. Sci. USA* **101** 23
[11] Buguin A, Brochard F and de Gennes P-G 2006 *Eur. Phys. J.* E **19** 31
[12] de Gennes P-G 2005 *J. Stat. Phys.* **119** 953
[13] de Boer M P, Luck D L, Ashurst W R, Maboudian R, Corwin A D, Walraven J A and Redmond J M 2004 *J. Microelectromech. Systems* **13** 63
[14] Eglin M, Eriksson M A and Carpick R W 2006 *Appl. Phys. Lett.* **88** 091913
[15] Dai Q, Vollmer R, Carpick R W, Ogletree D F and Salmeron M 1995 *Rev. Sci. Instrum.* **66** 5266
[16] Muser M H, Urbakh M and Robbins M O 2003 *Adv. Chem. Phys.* **126** 187
[17] Urbakh M *et al* 2004 *Nature* **430** 525
[18] Corwin A D and de Broer M P 2004 *Appl. Phys. Lett.* **84** 2451
[19] Ritter C *et al* 2005 *Phys. Rev.* B **71** 085405